16th World Conference on Earthquake, 16WCEE 2017

Santiago Chile, January 9th to 13th 2017

Paper N° 1952

Registration Code: S-T1464723460

DEVELOPMENT OF REAL-TIME TSUNAMI INUNDATION FORECAST METHOD USING A DENSE OFFSHORE OBSERVATION NETWORK

N. Yamamoto [1], S. Aoi[2], K. Hirata[2], W. Suzuki[2], T. Kunugi[2], H. Nakamura[2]

[1] *Researcher, National Research institute for Earth Science and Disaster Resilience (NIED), naotaka.yamamoto@bosai.go.jp*
[2] *National Research institute for Earth Science and Disaster Resilience (NIED)*

Abstract

We are developing a new algorithm for a real-time tsunami inundation forecast using the Seafloor Observation Network for Earthquakes and Tsunamis (S-net), which is now being constructed along the Japan Trench. In our algorithm, we first prepare the proposed Tsunami Scenario Bank (TSB), which contains offshore tsunami waveforms at the observatory location and the maximum tsunami height distributions, inundation depths, arrival times, etc. at the target coastal region. Ideally, TSB should contain tsunami information for all possible tsunami sources that may affect the target region, but it is impossible to prepare them in a finite time and computer resources. In this study, we tentatively construct the prototype of TSB with various tsunami source models in the Japan Trench region. We then quickly select several appropriate tsunami scenarios that can explain offshore tsunami observations by using multiple indices: correlation coefficient and two kinds of variance reductions. At that time, possible tsunami inundation information coupled with selected tsunami scenarios are forecast. To evaluate the propriety of our proposed method, we compare the coastal tsunami height distributions and/or tsunami inundation depth distributions of two paleotsunamis and those of corresponding selected tsunami scenarios.

Keywords: Real-time tsunami forecast; S-net; Multi-index

1. Introduction

A wide variety of methods for near-field tsunami forecasts have been proposed [1]. We define here a "real-time tsunami forecast" to derive the information required for evacuation before the first arrival of a tsunami on the coast. In Japan, a real-time tsunami forecast using the hypocenter location and the earthquake magnitude determined from land-based seismological observation has been operating by the Japan Meteorological Agency (JMA) since 1999[2, 3]. This is used as an initial forecast because it can be issued very quickly. However, it has large uncertainties, because land-based seismic observation alone cannot constrain the hypocenter location and the magnitude of subduction zone earthquakes. Accordingly, a more accurate real-time tsunami forecast method using fault geometry information and the average amount of slip determined by the Global Navigation Satellite System (GNSS) was proposed [4]. Because the fault model is obtained from GNSS data within a few minutes after an earthquake occurs, it is possible to replace the initial forecast information with more accurate information [1]. The Pacific Marine Environmental Laboratory (PMEL) of the National Oceanic Atmospheric Administration (NOAA) extremely succeeded in far-field tsunami forecasting based on recorded tsunami data taken by the Deep-ocean Assessment and Reporting of Tsunamis (DART) system [5]. For near-field tsunami forecast, the method to estimate the best tsunami source model by inversion analysis of tsunami waveform data from ocean-bottom pressure gauges was proposed [6]. In their method, arrival times and tsunami amplitudes at the coasts are forecast by linearly combining pre-calculated Green's functions. However, obtaining direct measurements of tsunamis requires more time to detect tsunami signals than obtaining seismic wave or real-time GNSS data. Attempting a breakthrough, the correlation between offshore and coastal tsunami heights is investigated by using ocean-bottom pressure data from the Dense Oceanfloor Network system for Earthquakes and Tsunamis (DONET) observation array [7, 8]. They successfully forecast the coastal tsunami height within 10 min after the occurrence of an earthquake by concentrating on predicting the tsunami scale. In addition, the rapid method to estimate tsunami source location using a dense offshore observation network was proposed [9]. They claimed the tsunami source location could be estimated within a few minutes after the occurrence of an earthquake by using tsunami centroid location (TCL). Although direct measurements of tsunamis are used in their method, the required estimation time is comparable to that achieved using real-time GNSS data. It is possible to replace the earthquake location and magnitude with the tsunami source location [9] and the tsunami scale [7] for the initial tsunami warning. For a real-time tsunami inundation forecast, some researchers have proposed new methods that use on-demand forward simulations with inverted tsunami source models [10, 11, 12]. However, these methods require enormous computer power, hence the coastal region to be forecast is limited. To achieve a real-time tsunami inundation forecast on high-resolution topography, a new method is proposed [13]. In their method, the best-matched tsunami scenario selected by comparing pre-calculated tsunami waveforms and synthetic tsunami waveforms calculated using forecasted tsunami source information is forecast.

We started to develop a real-time tsunami inundation forecast system [14] using the Seafloor Observation Network for Earthquakes and Tsunamis (S-net) along the Japan Trench [15, 16], which is now being constructed by the National Research Institute for Earth Science and Disaster Resilience (NIED). As a part of this system development, we propose a new approach for real-time tsunami inundation forecasts that uses only tsunami data obtained by offshore ocean-bottom pressure gauges without the influence of estimation errors in the hypocenter location or the earthquake magnitude determined by seismological observations [17, 18]. In our algorithm, the most important concept is involving any type and/or form uncertainties in the tsunami forecast, which cannot be dealt with any of standard linear/nonlinear least square approaches. We first prepare a Tsunami Scenario Bank (TSB), which contains offshore tsunami waveforms at the observatory location and tsunami prediction information at the target coastal region, such as maximum tsunami height distribution, inundation depths, arrival times, etc. calculated from any possible tsunami source. If we could consider all possible tsunami scenarios, the tsunami forecast would be highly precise. However, the number of tsunami scenarios that can be pre- pared is limited due to finite time and computing resources. In other words, a tsunami scenario selected from pre-calculated tsunami scenarios cannot always make correct predictions for an entire coastal region. Therefore, we select dozens of tsunami scenarios that can explain offshore observation data by using multiple indices: correlation coefficient and two variance reductions, whose L2-norm part is normalized either by observations or calculations. At that time, possible tsunami prediction information coupled with selected scenarios are forecast.

In this paper, to determine whether our method can select appropriate tsunami scenarios, we prepare the fault models based on some known paleotsunamis that affected the eastern coast of Japan. We confirm the propriety of our method by comparison between tsunami prediction information of "pseudo observation" simulated as paleotsunamis and those of calculation selected from the TSB.

2. Matching method

We define here a method for comparing the observed waveform O($\mathbf{r}_i$,t) and the pre-calculated waveform C($\mathbf{r}_i$,t) registered in the TSB, for the i-th observation unit at a position $\mathbf{r}_i$ after a time t has elapsed following an earthquake.

2.1 Three indices

We define three new indices by adding time-shift τ and weight w($\mathbf{r}_i$) to the previous definitions [18]: the correlation coefficient and two kinds of variance reductions, to compare O($\mathbf{r}_i$,t) to C($\mathbf{r}_i$,t-τ), where C($\mathbf{r}_i$,t-τ) is the time-shifted calculated tsunami waveform, and τ is the amount of time-shift. The correlation coefficient R(t,τ), which is a function of time t, is defined as follows:

$$R(t,\tau)=\frac{\sum_{i=1}^{n} w(\mathbf{r}_i)\,O(\mathbf{r}_i,t)\,C(\mathbf{r}_i,t-\tau)}{\sqrt{\sum_{i=1}^{n} w(\mathbf{r}_i)\,O^2(\mathbf{r}_i,t)}\sqrt{\sum_{i=1}^{n} w(\mathbf{r}_i)\,C^2(\mathbf{r}_i,t-\tau)}}, \tag{1}$$

where n is the number of observation stations and w($\mathbf{r}_i$) is weight for the i-th observation station at $\mathbf{r}_i$. Equation (1) indicates that R(t,τ) is the cosine of the angle formed by two n-dimensional vectors, O($\mathbf{r}_i$,t) and C($\mathbf{r}_i$,t-τ), i.e., R(t,τ) ranges from -1 to 1. R(t,τ) is expected to be sensitive to the tsunami source location, because R(t,τ) strongly depends on the difference between spatial distribution of O($\mathbf{r}_i$,t) and C($\mathbf{r}_i$,t-τ). However, R(t,τ) is close to 1 when their spatial distributions are similar, even though the amplitudes of O($\mathbf{r}_i$,t) and C($\mathbf{r}_i$,t-τ) are very different.

Next, we also define the new variance reductions to discriminate between good and bad matching accuracy. In this study we use two variance reductions, VRO(t,τ) and VRC(t,τ), as functions of time t normalized by the L2-norm of either the observed waveform O($\mathbf{r}_i$,t) or the calculated waveform C($\mathbf{r}_i$,t-τ), as follows:

$$VRO(t,\tau)=1-\frac{\sum_{i=1}^{n} w(\mathbf{r}_i)\left(O(\mathbf{r}_i,t)-C(\mathbf{r}_i,t-\tau)\right)^2}{\sum_{i=1}^{n} w(\mathbf{r}_i)\,O^2(\mathbf{r}_i,t)} \tag{2}$$

$$VRC(t,\tau)=1-\frac{\sum_{i=1}^{n} w(\mathbf{r}_i)\left(O(\mathbf{r}_i,t)-C(\mathbf{r}_i,t-\tau)\right)^2}{\sum_{i=1}^{n} w(\mathbf{r}_i)\,C^2(\mathbf{r}_i,t-\tau)}. \tag{3}$$

As defined by Eqs. (2) and (3), both variance reductions become 1 when O($\mathbf{r}_i$,t) equals C($\mathbf{r}_i$,t-τ), i.e., variance reductions of 1 indicate the best matches. These values become smaller as O($\mathbf{r}_i$,t) becomes more different from C($\mathbf{r}_i$,t-τ). Therefore, VRO(t,τ) and VRC(t,τ) range from -∞ to 1.

2.2 Waveform conversion

We use the maximum value of the absolute values of the observed waveforms O($\boldsymbol{r}_i$,t) [18], defined as follows:

$$O(\mathbf{r}_i, t) = \max_{t' \le t}\left(\left|O_{original}(\mathbf{r}_i, t')\right|\right). \quad (4)$$

The converted values become constant after a sufficient time lapse following an earthquake. We also apply the same conversion to the calculated waveform C($\boldsymbol{r}_i$,t) as follows:

$$C(\mathbf{r}_i, t) = \max_{t' \le t}\left(\left|C_{original}(\mathbf{r}_i, t')\right|\right). \quad (5)$$

When we compare the converted waveforms O($\boldsymbol{r}_i$,t) and C($\boldsymbol{r}_i$,t-τ), the correlation coefficient R(t,τ) never becomes negative, i.e., R(t,τ) ranges from 0 to 1.

3. Construction of a tentative TSB

In this study, we set up 1,890 tsunami source models in the Japan Trench region, which can affect the Pacific coast of eastern Japan [18]. The models, which were previously prepared for a probabilistic tsunami hazard assessment [19], are used to construct a tentative TSB (hereafter TSB-A). We then calculate synthetic offshore tsunami waveforms $\eta(\boldsymbol{r}_i,t)$ for 150 statins of S-net by solving nonlinear long-wave equations using a staggered leapfrog finite-difference scheme. In these calculations, we assume that the sea surface displacement is the same as the vertical seafloor displacement of coseismic crustal deformation due to an earthquake, and the sea surface displacement is immediately completed at time t=0. The calculated tsunami waveform $\eta(\boldsymbol{r}_i,t)$ are converted to ocean-bottom hydrostatic pressure changes C($\boldsymbol{r}_i$,t) as follows:

$$C(\mathbf{r}_i, t) = \rho g\left(\eta(\mathbf{r}_i, t) - \eta_0(\mathbf{r}_i)\right), \quad (6)$$

where ρ is the average density of seawater, g is the gravitational acceleration, and $\eta_0(\boldsymbol{r}_i)$ is the initial sea surface displacement, which is the same as the permanent seafloor deformation calculated by Okada's formula [20]. We also assume that the hydrostatic ocean-bottom pressure, which is proportional to the total water depth, does not change during an earthquake, i.e., C($\boldsymbol{r}_i$,t=0)=0, because the ocean-bottom pressure gauges are displaced by the seafloor deformation, which is equal to the sea surface displacement. Finally, we register the calculated waveform C($\boldsymbol{r}_i$,t) with its fault model and the maximum coastal tsunami heights along the Pacific coast of Kanto, Tohoku, and Hokkaido.

To extend the previous TSB, we additionally prepare 3,282 tsunami source models in the Japan Trench region. These models, which are mechanically defined by simple rectangle fault models to prepare a large amount of tsunami source models, are used to construct another tentative TSB (hereafter TSB-B). We then calculate synthetic offshore tsunami waveform $\eta(\boldsymbol{r}_i,t)$ for 150 statins of S-net and coastal tsunami heights and tsunami inundation depth distributions with the same procedure for constructing of TSB-A but for the Pacific coast of Chiba prefecture.

4. Case studies and evaluations

To investigate whether it is possible to select appropriate tsunami scenarios from the tentative TSBs by using the three indices defined in Eqs. (1), (2), and (3) with the maximum absolute values defined in Eqs. (4) and (5) with the assumption of w($\boldsymbol{r}_i$) = 0. In this study, we also assume that synthetic observed waveforms, which are simulated by the paleotsunamis, are "pseudo observation" waveforms because actual tsunami observation data on the S-net have not yet been recorded. We then examine the selected tsunami scenarios by comparing the maximum coastal tsunami height distributions and/or tsunami inundation depth distributions of the pseudo observation scenarios and the selected tsunami scenarios. In this section, we describe the results of these examinations.

4.1 Examination of 2011 Tohoku earthquake tsunami

As the pseudo observation scenario, we calculate tsunami waveforms by using the slip distribution of the 2011 Tohoku earthquake, suggested by Cabinet Office [21]. Our multi-index method selects 25 tsunami scenarios under the criteria of VRO (t=7 min,τ) >= 0.0, VRC (t=7 min,τ) >= 0.0, and R (t=7 min,τ) >= 0.7. Fig. 1 plots the selected scenarios on the VRO-VRC diagram [18] at t=7 min with τ=3 min. As shown in Fig. 1, the values of VRC (t=7 min, τ=3 min) for many unselected tsunami scenarios are strongly negative. This indicates that the 2011 Tohoku earthquake tsunami is close to the maximum class of tsunami scenarios registered in the tentative TSB-A, i.e., many tsunami scenarios registered in the TSB-A are rejected due to underestimations because VRC is sensitive to underestimation of C($\boldsymbol{r}_i$,t) with respect to O($\boldsymbol{r}_i$,t) [18]. Fig. 2 is a color contour map for R (t=7 min, τ=3 min) plotted at the centroid location of the slip distribution of fault models registered in the TSB-A. The figure suggests that the calculated scenarios with R(t,τ) close to zero are far from the location of the fault model of the pseudo observation scenario, i.e., R(t,τ) is sensitive to the tsunami source location. The figure also shows that the distribution of R(t,τ) values is approximately consistent with the fault slip distributions obtained by inversions.

Fig. 3 shows evaluations for maximum coastal tsunami height distribution of the 2011 Tohoku earthquake. The left figure indicates maximum coastal tsunami height distribution of the pseudo observation and 25 selected tsunami scenarios. The right figure plots the selected tsunami scenarios on the coastal VRO-VRC diagram. We confirm that our method can select tsunami scenarios appropriately for the 2011 Tohoku earthquake, because the selected tsunami scenarios satisfy coastal VRO > 0.75, coastal VRC > 0.57, and coastal R > 0.87.

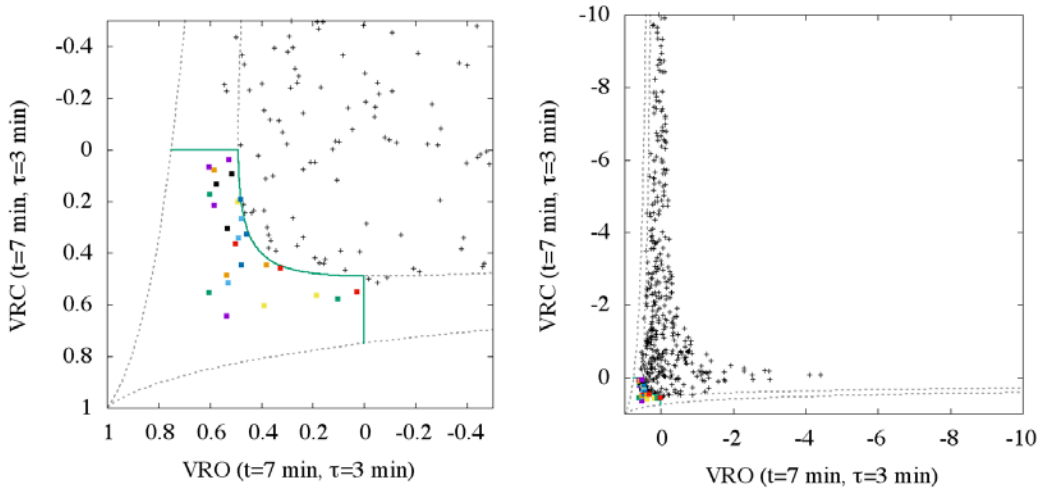

Fig. 1 – Offshore comparisons at t=7 min after the occurrence of the 2011 Tohoku earthquake with time shift τ=3 min. The left figure shows the close-up plot around criteria and the right figure shows the wide view of the VRO-VRC diagram, respectively [18]. The area surrounded by the green curves indicates the applied criteria, VRO (t=7 min,τ) >= 0.0, VRC (t=7 min,τ) >= 0.0, and R (t=7 min,τ) >= 0.7 and the dashed curves indicate R=1. All possible pairs of all scenarios are restricted to the range between R=1.0 and R=0.0. The left-bottom corner of (1,1) in the VRO-VRC diagram indicates that C($\boldsymbol{r}_i$,t) is completely matched with O($\boldsymbol{r}_i$,t). The colored squares represent the selected tsunami scenarios and the grey crosses represent the unselected tsunami scenarios. The best-matched scenario that is the closest to (1,1) and represented by the purple square is shown at (VRO,VRC) = (0.536,0.641) with R=0.804.

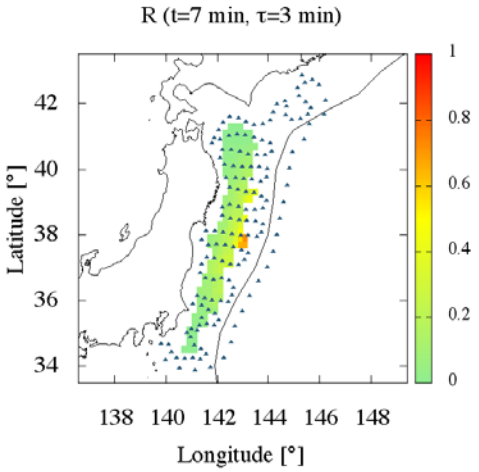

Fig. 2 – Color contour map of R (t=7 min, τ=3 min) for the 2011 Tohoku earthquake. R (t=7 min, τ=3 min) values are plotted at the centroid location of the slip distribution of each fault model registered in the TSB-A.

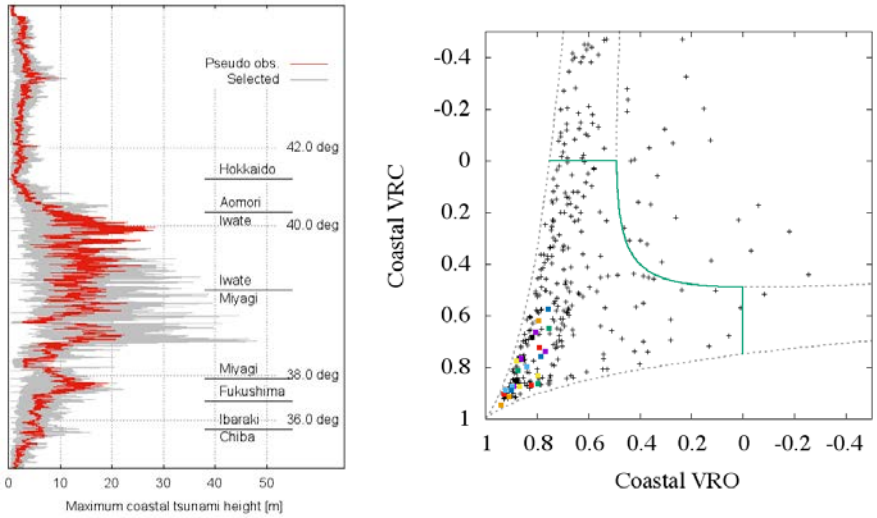

Fig. 3 – Evaluation for maximum coastal tsunami height distributions of the selected tsunami scenarios for the 2011 Tohoku earthquake tsunami. The left figure compares maximum coastal tsunami height distributions of the pseudo observation (red line) along the target coastaline with 25 selected tsunami scenarios (grey lines) in the background. The right figure is coastal VRO-VRC diagram by comparing maximum coastal tsunami height distributions for the corresponding tsunami scenarios. The colored squares indicate the selected tsunami scenarios with colors that are the same as those in Fig. 1.

4.2 Examination of 1677 Enpo Boso-oki earthquake tsunami

As the next pseudo observation scenario, we calculate tsunami waveforms by using the slip distribution of the 1677 Enpo Boso-oki earthquake [22] (Fig. 4). We use the same thresholds: VRO (t=5 min) >= 0.0, VRC (t=5 min) >= 0.0, and R (t=5 min) >= 0.7 with τ=0 because fault model does not include dynamic rupture process. Fig. 5 plots the selected scenarios on the VRO-VRC diagram at t=5 min. From the right figure of Fig. 5, which shows a wider range of the VRO-VRC diagram, we can see that many unselected tsunami scenarios are plotted along the R = 0.0 curve, i.e., many tsunami scenarios registered in the TSB-B do not satisfy the threshold R >= 0.7.

Fig. 6 shows evaluations for maximum coastal tsunami height distribution of the 1677 Enpo Boso-oki tsunami. The right figure indicates maximum coastal tsunami height distribution of the pseudo observation (red line) and the best-matched scenario (purple line) with 24 selected tsunami scenarios (grey lines). Fig. 7 shows an example of inundation depth distribution to compare the 1677 Enpo Boso-oki tsunami and the best-matched scenario. From these figures, we confirm that our method can select tsunami scenarios appropriately for the 1677 Enpo Boso-oki earthquake.

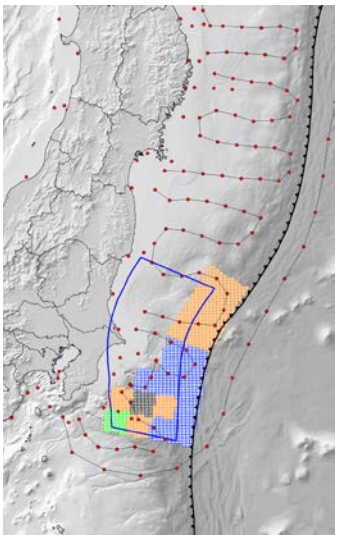

Fig. 4 – Slip distribution of the 1677 Enpo Boso-oki tsunami. The blue polygon indicates the fault model of the best-matched tsunami scenario. The red cirlces connected by grey lines show the locations of the ocean-bottom pressure gauges of the S-net.

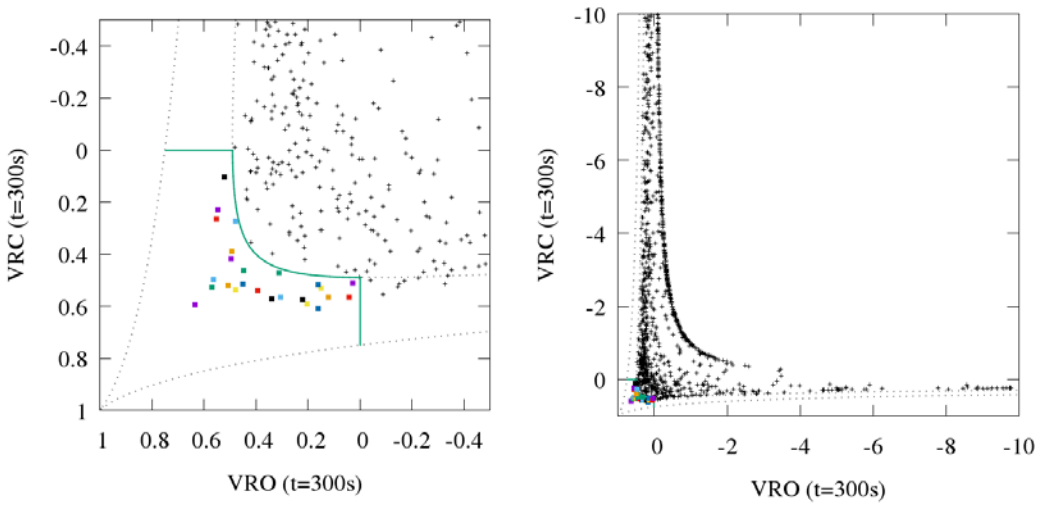

Fig. 5 – Offshore comparisons at 5 min after the occurrence of the 1677 Enpo Boso-oki tsunami. The left figure shows the close-up plot around criteria and the right figure shows the wide view of the VRO-VRC diagram [18], respectively (see also the caption of Fig. 1). The area surrounded by the green curves indicates the applied criteria, VRO (t=5 min) >= 0.0, VRC (t=5 min) >= 0.0, and R (t=5 min) >= 0.7. The colored squares represent the selected tsunami scenarios and the grey crosses represent the unselected tsunami scenarios. The best-matched scenario that is represented by the purple square is shown at (VRO,VRC) = (0.634,0.594) with R=0.808.

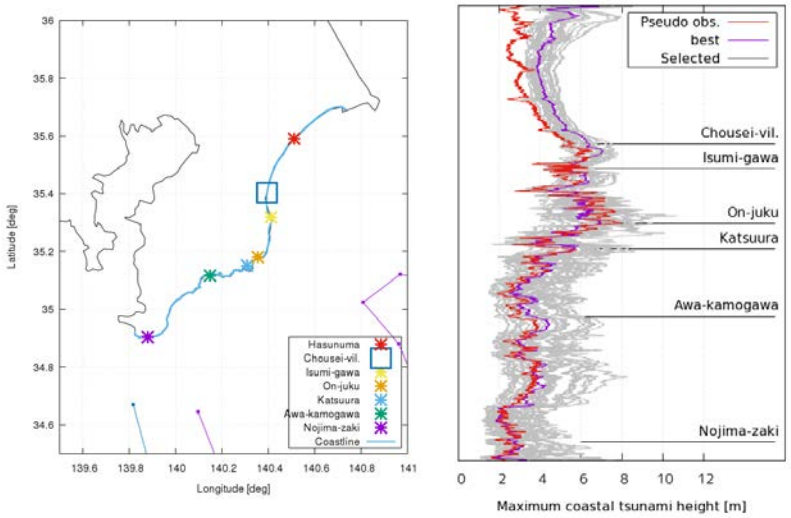

Fig. 6 – Evaluation for maximum coastal tsunami height distributions for the 1677 Enpo Boso-oki tsunami. The left figure shows the target coastline (blue line). The ritht figure compares maximum coastal tsunami height distributions of the pseudo observation (red line) and the best-matched scenario (purple line) along the target coastaline with 24 selected tsunami scenarios (grey lines) in the background.

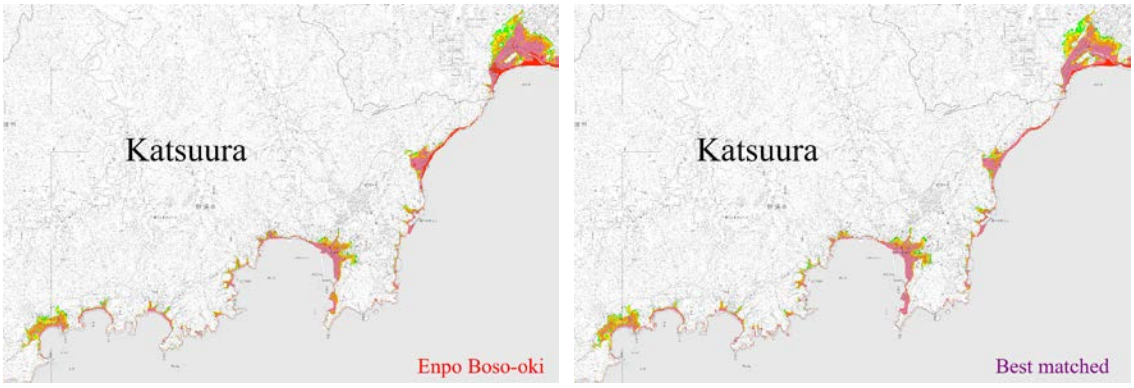

Fig. 7 – Comparison between inundation depth distributions for the 1677 Enpo Boso-oki tsunami (left) and the best-matched scenario (right) shown in purple square and line in Fig.5 and 6, respectively.

5. Conclusions

We extended the multi-index method for a real-time tsunami inundation forecast, which selects appropriate tsunami scenarios by comparing offshore observed waveforms and pre-calculated waveforms registered in the Tsunami Scenario Bank (TSB). To evaluate the propriety of our proposed method, we applied our method to the 2011 Tohoku earthquake tsunami and the 1677 Enpo Boso-oki tsunami. From these examinations, we confirmed that appropriate tsunami scenarios could be selected by using the three indices, which are two kinds of variance reductions and a correlation coefficient, comparing between the pseudo observation and calculated offshore waveforms. We showed that our method could select appropriate tsunami scenarios whose maximum coastal tsunami height distributions and inundation depth distributions are close to those of the pseudo observation scenario by comparing offshore waveforms.

6. Acknowledgements

This work was partially supported by the Council for Science, Technology and Innovation (CSTI) through the Cross-ministerial Strategic Innovation Promotion Program (SIP), titled “Enhancement of societal resiliency against natural disasters” (Funding agency: JST).

7. References

[1] Tsushima H, Ohta Y (2014): Review on near-field tsunami fore- casting from offshore tsunami data and onshore GNSS data for tsunami early warning. *Journal of Disaster Research*, **9** (3), 339-357.

[2] Tatehata H (1997): The new tsunami warning system of the Japan Meteorological Agency. *In Perspectives on Tsunami Hazard Reduction*, 175-188.

[3] Kamigaichi O (2009): Tsunami forecasting and warning. *In Encyclopedia of Complexity and Systems Science*, 9592-9618.

[4] Blewitt G, Hammond WC, Kreemer C, Plag HP, Stein S, Okal E (2009): GPS for real-time earthquake source determination and tsunami warning systems. *Journal of Geodesy*, **83** (3-4), 335-343.

[5] Titov VV, Gonzalez FI, Bernard EN, Eble MC, Mofjeld HO, Newman JC, Venturato AJ (2005): Real-time tsunami forecasting: Challenges and solutions, *In Developing tsunami-resilient communities*, 41-58.

[6] Tsushima H, Hino R, Fujimoto H, Tanioka H, Imamura F (2009): Near-field tsunami forecasting from cabled ocean bot- tom pressure data. *Journal of Geophysical Research: Solid Earth*, B06309, **114** (B6).

[7] Baba T, Takahashi N, Kaneda Y (2014): Near-field tsunami amplification factors in the kii peninsula, japan for Dense Ocean-floor Network for Earthquakes and Tsunamis (DONET), *Marine Geophysical Research*, **35**(3), 319-325.

[8] Kaneda Y, Kawaguchi K, Araki E, Sakuma A, Matsumoto H, Nakamura T, Kamiya S, Ariyoshi K, Baba T, Ohori M, Hori T (2009): Dense Ocean floor Network for Earthquakes and Tsunamis (DONET) -development and data application for the mega thrust earthquakes around the Nankai trough-. *In Abstract S53A-1453 presented at 2009 Fall Meeting, AGU*, San Francisco, CA.

[9] Yamamoto N, Hirata K, Aoi S, Suzuki W, Nakamura H, Kunugi T (2016): Rapid estimation of tsunami source centroid location using a dense offshore observation network. *Geophysical Research Letters*, **43** (9), 4263-4269.

[10] Tatsumi D, Tomita T (2013): Development and implementation of real-time tsunami inundation prediction method [in Japanese with English abstract]. *Journal of Japan Society of Civil Engineers, Ser. B2 (Coastal Engineering)*, **69** (1), 34-47.

[11] Koshimura S, Hino R, Ohta Y, Kobayashi H, Musa A, Murashima Y (2014): Real-time tsunami inundation forecasting and damage mapping towards enhancing tsunami disaster resiliency. *In Abstract MH23B-05 presented at 2014 Fall Meeting*, San Francisco, CA.

[12] Oishi Y, Imamura F, Sugawara D (2015): Near-field tsunami inundation forecast using the parallel TSUNAMI-N2 model: Application to the 2011 Tohoku-Oki earthquake combined with source inversions. *Geophysical Research Letters*, **42** (4), 1083-1091.

[13] Gusman AR, Tanioka Y, MacInnes BT, Tsushima H (2014): A methodology for near-field tsunami inundation forecasting: Application to the 2011 Tohoku tsunami. *Journal of Geophysical Research: Solid Earth*, **119** (11), 8186-8206.

[14] Aoi S, Yamamoto N, Suzuki W, Hirata K, Nakamura H, Kunugi T, Kubo T, Maeda T (2015): Development of real-time tsunami inundation forecast using ocean bottom tsunami networks along the Japan trench. *In Abstract NH13E-04 presented at 2015 Fall Meeting*, San Francisco.

[15] Kanazawa T, Kunugi T, Noguchi S, Sekiguchi S, Shiomi K, Aoi S, Okada Y, Shinohara M, Yamada T (2012): Ocean bottom seismic and tsunami network along the Japan trench. *In Abstract HDS26-06 presented at Japan Geoscience Union Meeting 2012*, Makuhari, Japan.

[16] Uehira K, Kanazawa T, Mochizuki M, Fujimoto H, Noguchi S, Shinbo T, Shiomi K, Kunugi T, Aoi S, Matsumoto T, Sekiguchi S, Okada Y, Shinohara M, Yamada T (2015): Seafloor observation Network for Earthquakes and Tsunamis

along the Japan trench (S-net), *In Abstract IUGG-3547 presented at 2015 26th General Assembly of IUGG*, Prague, Czech Republic.

[17] Yamamoto N, Aoi S, Hirata K, Suzuki W, Kunugi T, Nakamura H (2015): A new algorithm for real-time near-field tsunami inundation forecast using a dense offshore tsunami observation network. *In Abstract IUGG-2320 presented at 2015 26th General Assembly of IUGG*, Prague, Czech Republic.

[18] Yamamoto N, Aoi S, Hirata K, Suzuki W, Kunugi T, Nakamura H (2016): Multi-index method using offshore ocean-bottom pressure data for real-time tsunami forecast. *Earth, Planets and Space*, 68 (1), 128.

[19] Hirata K, Fujiwara H, Nakamura H, Osada M, Ohsumi T, Morikawa N, Kawai S, Aoi S, Yamamoto N, Matsuyama H, Toyama N, Kito T, Murashima Y, Murata Y, Inoue T, Saito R, Akiyama S, Korenaga M, Abe Y, Hashimoto N (2014): Nationwide tsunami hazard assessment project in Japan. *In Abstract NH12A-03 presented at 2014 Fall Meeting, AGU*, San Francisco, CA.

[20] Okada Y (1985): Surface deformation due to shear and tensile faults in a half-space. *Bulletin of the Seismological Society of America*, **75** (4), 1135-1154.

[21] Government of Japan Cabinet Offce (2012): Tsunami source model of 2011 Tohoku earthquake tsunami (in Japanese) http://www.bousai.go.jp/jishin/nankai/model/12/pdf/sub 1.pdf, Accessed 28 Dec 2015.

[22] Takeuchi H, Fuji R, Mimura N, Imamura F, Satake K, Tsuji Y, Hochi K, Matsuura T (2007): Survey of run-up height of Empo Boso-oki earthquake tsunami on the coast from Chiba prefecture to Fukushima prefecture, *Hist. Earthquake*, **22**, 53-59.